Neuron, Vol. 35, 1057–1066, September 12, 2002, Copyright ©2002 by Cell Press

A Divergent Pattern of Sensory Axonal Projections Is Rendered Convergent by Second-Order Neurons in the Accessory Olfactory Bulb

Karina Del Punta,[1] Adam Puche,[2] Niels C. Adams,[1,4] Ivan Rodriguez,[1,5] and Peter Mombaerts[1,3]
[1]The Rockefeller University
1230 York Avenue
New York, New York 10021
[2]University of Maryland
Department of Anatomy and Neurobiology
685 West Baltimore Street
Baltimore, Maryland 21201

Summary

The mammalian vomeronasal system is specialized in pheromone detection. The neural circuitry of the accessory olfactory bulb (AOB) provides an anatomical substrate for the coding of pheromone information. Here, we describe the axonal projection pattern of vomeronasal sensory neurons to the AOB and the dendritic connectivity pattern of second-order neurons. Genetically traced sensory neurons expressing a given gene of the V2R class of vomeronasal receptors project their axons to six to ten glomeruli distributed in globally conserved areas of the AOB, a theme similar to V1R-expressing neurons. Surprisingly, second-order neurons tend to project their dendrites to glomeruli innervated by axons of sensory neurons expressing the same V1R or the same V2R gene. Convergence of receptor type information in the olfactory bulb may represent a common design in olfactory systems.

Introduction

The sense of smell endows animals with the ability to deduce information about the chemical composition of the external world. Many mammals have two distinct olfactory systems to recognize and process this information: the main olfactory and the vomeronasal systems. The main olfactory system is responsible for detecting an enormous variety of volatile airborne odorants and translating this information into cognitive and emotional responses (Firestein, 2001). In contrast, the vomeronasal system is thought to be involved mainly, although not exclusively (Sam et al., 2001), in the detection of pheromones (Halpern, 1987; Keverne, 1999). It responds to a more specific set of stimuli (Holy et al., 2000; Leinders-Zufall et al., 2000), which elicit neuroendrocine effects and instinctive behaviors related to reproduction and social dominance.

The olfactory and vomeronasal systems have segregated anatomical organizations. Olfactory sensory neurons (OSNs) of the main olfactory epithelium (MOE) in the nasal cavity project their axons to the main olfactory bulb (MOB), where they innervate glomeruli, globose condensations of neuropil. Within glomeruli, OSN axons synapse with the dendrites of second-order neurons, the mitral/tufted cells, which in turn project their axons to the primary olfactory cortex and other regions of the brain. Vomeronasal sensory neurons (VSNs) reside within the epithelium of a blind capsule, the vomeronasal organ (VNO), and project their axons to a specialized region of the dorsocaudal olfactory bulb, the accessory olfactory bulb (AOB). VSN axons in the AOB also innervate glomeruli, but these structures are smaller and less defined than MOB glomeruli. VSN axons also synapse with the apical dendrites of mitral cells, which project to the medial amygdala and hypothalamic nuclei, thus bypassing the primary olfactory cortex (Halpern, 1987).

Recent molecular and genetic studies have shed light on the logic of information coding in the olfactory system. In mammals, each OSN expresses one of >1000 odorant receptor (OR) genes (Buck and Axel, 1991; Malnic et al., 1999). In contrast to their scattered distribution in the sensory epithelium, OSNs expressing a given OR send convergent axonal projections to a few spatially conserved glomeruli in the MOB (Ressler et al., 1994; Vassar et al., 1994; Mombaerts et al., 1996; Mombaerts, 2001) (Figure 1A). A mitral cell in the MOB projects its single apical dendrite to a single glomerulus. This organization supports a model of olfactory coding in which odor quality is encoded by a specific combination of activated mitral cells, each of which receives inputs from OSNs that express the same OR.

Much less is known about the circuit organization of the vomeronasal system. This sensory system exhibits a distinct anatomical and molecular dichotomy (Figure 1A) whose biological significance remains enigmatic. Two subdivisions of VSNs are distinguished by the location of the cell body within the vomeronasal epithelium, the class of vomeronasal receptor expressed, the type of G protein subunit expressed (Halpern et al., 1995; Berghard and Buck, 1996), and the site of termination of axons in the AOB (Jia and Halpern, 1996; Yoshihara et al., 1997). VSNs whose cell bodies are situated apically coexpress the V1R class of vomeronasal receptors (VRs) (Dulac and Axel, 1995; Del Punta et al., 2000; Rodriguez et al., 2002) with $G\alpha_{i2}$ and project their axons to the rostral half of the AOB. In contrast, VSNs with more basally located cell bodies coexpress the V2R class of receptors (Herrada and Dulac, 1997; Matsunami and Buck, 1997; Ryba and Tirindelli, 1997) with $G\alpha_o$ and project their axons to the caudal half of the AOB. The V1R and V2R gene families encode seven-transmembrane domain receptors, which have no significant sequence homology with each other or with ORs. In the AOB, the innervation of a single mitral cell is restricted to either the rostral or the caudal AOB (Jia and Halpern, 1997; von Campenhausen et al., 1997). The two segregated pathways are thought to respond to different stimuli and mediate differential behaviors (Brennan et al., 1999; Dudley and Moss, 1999; Kumar et al., 1999; Halem et al., 2001).

How is the initial event of chemoreception translated

[3]Correspondence: peter@rockefeller.edu
[4]Present address: Regeneron Pharmaceuticals, Inc., 777 Old Saw Mill River Road, Tarrytown, New York 10591.
[5]Present address: Department of Zoology and Animal Biology, Sciences III, University of Geneva, 1211 Geneva 4, Switzerland.

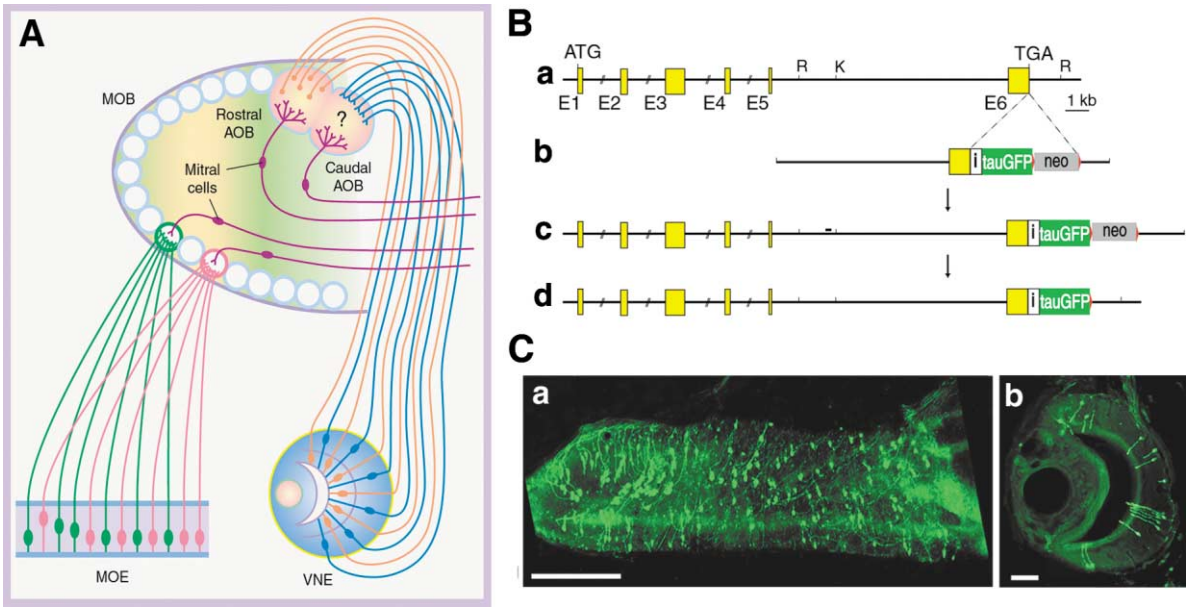

Figure 1. Genetic Approach to Visualizing V2R-Expressing Neurons

(A) Anatomical organization of axonal projections of sensory neurons of the main and vomeronasal sytems. Schematic representation of OSNs and VSNs projecting their axons to the MOB and AOB, respectively. OSNs expressing the same OR, shown as pink and green for two different neuronal populations, project their axons to a single glomerulus in each half of a MOB. Each mitral cell in the MOB has a single apical dendrite, innervating a single glomerulus. In contrast, VSNs expressing a given V1R (orange) project their axons to multiple, smaller glomeruli in the AOB. The pattern of projections of VSNs expressing a given V2R (blue) is unknown. Mitral cells in the AOB have apical dendrites innervating multiple glomeruli.

(Ba–Bd) Targeted mutagenesis of the *V2r1b* locus. (Ba) Wild-type *V2r1b* locus. The yellow boxes represent the coding exons. Restriction sites are indicated for EcoRI (R) and KpnI (K). ATG is the start codon; TGA is the stop codon. (Bb) *V2r1b-IRES-tauGFP-LNL* targeting vector. The white box labeled "i" represents the *IRES* sequence, the green box represents the coding sequence of tauGFP, and the gray box labeled "neo" represents the *neo*-selectable marker *LNL* flanked by loxP sites (indicated by red triangles). (Bc) *V2r1b* locus after homologous recombination with the *V2r1b-IRES-tauGFP-LNL* targeting vector. The probe used to detect homologous recombination in Southern blots is represented as a small horizontal bar in the middle. (Bd) *V2r1b* locus after Cre-mediated excision of the *neo* cassette, which leaves a single *loxP* site behind. This is the targeted mutation studied here.

(Ca and Cb) *V2r1b*-expressing neurons in the VNO. (Ca) Whole-mount lateral view of the VNO. Anterior is to the left, dorsal is to the top. Neurons expressing *V2r1b* also express GFP and are fluorescent green. Scale bar, 500 μm. (Cb) Cross-section through the VNO. *V2r1b*-expressing neurons are situated in the basal layer of the epithelium. Cell bodies, dendrites, and axons can be discerned. Scale bar, 100 μm.

to create a neural representation of the stimuli in the brain? Analogous to OSNs, VSNs appear to express a single V1R or V2R gene, but exceptions exist (Martini et al., 2001). VSNs expressing a particular VR have no obvious distribution throughout the VNE. However, in contrast to the convergence onto one or a few glomeruli by OSN axons in the MOB, axons from VSNs expressing a given V1R innervate multiple (15–30) smaller glomeruli in the rostral half of the AOB (Belluscio et al. 1999; Rodriguez et al., 1999) (Figure 1A). Glomeruli are distributed in globally conserved areas in the AOB of different individuals, although their precise individual location is variable. The pattern of axonal projections of neurons expressing V2R genes to the caudal AOB has not yet been described.

How is this complex glomerular pattern in the AOB processed by the mitral cells? It has been known for nearly a century that second-order neurons in the AOB have a qualitatively different organization than those of the MOB: apical dendrites of AOB mitral cells elaborate an extensive branching pattern such that each cell innervates multiple glomeruli (Ramon y Cajal, 1911; Takami and Graziadei, 1990, 1991). The peculiar anatomical relationship between glomeruli and mitral cells in the AOB raises the question as to how mitral cell connectivity relates to glomerular receptor identity. Whether a mitral cell innervates glomeruli with the same or different receptor specificities has implications for our understanding of the coding of chemosensory information in the AOB.

To determine the wiring logic of the AOB, we here trace with a genetic technique the axonal projections of neurons expressing a given V2R, and we describe the dendritic connectivity pattern between mitral cells and glomeruli with the same V1R or V2R receptor specificity (Figure 1A). First, we show that VSNs expressing the *V2r1b* gene project their axons to six to ten glomeruli that reside in globally conserved areas within the caudal AOB. These glomeruli appear to be exclusive targets of axons from *V2r1b*-expressing neurons. Thus, based on this example, neurons expressing *V1R* or *V2R* genes rely on similar strategies to organize the input of information at the glomerular level, although they constitute two anatomically segregated compartments using receptors without significant sequence homology. Second, injection of lipophilic tracers into individual genetically labeled glomeruli reveals that mitral cells connect to multiple glomeruli innervated by neurons expressing the same V1R or V2R. Thus, the divergent pattern of projec-

tions of VSNs neurons in the AOB is resolved by dendritic convergence of the second-order neurons.

Results

Visualizing *V2r1b*-Expressing Sensory Neurons

The genomic structure of the *V2r1b* gene, a member of the V2R class of vomeronasal receptors (Ryba and Tirindelli, 1997), is shown in Figure 1B. The coding sequence spans six exons: five exons (E1 to E5) encode the long extracellular domain, and a single exon (E6) codes for the transmembrane domain. The predicted amino acid sequence of V2r1b shares 98.4% identity with its closest homolog, V2R1.

To visualize *V2r1b*-expressing VSNs and their axonal projections to the AOB, we generated a targeted mutation in the *V2r1b* locus that results in cotranslation of tauGFP along with V2r1b from a bicistronic message. An IRES-tauGFP-LNL cassette was introduced immediately after the stop codon of the *V2r1b* coding sequence (Figure 1B). In this well-established design (Rodriguez et al., 1999; Zheng et al., 2000; Strotmann et al., 2000; Potter et al., 2001; Bozza et al., 2002; Treloar et al., 2002), the fluorescent label is present in axons and axon terminals of *V2r1b*-expressing VSNs. V2r1b-IRES-tauGFP mice are abbreviated as V2R-GFP mice.

To investigate the distribution of *V2r1b*-expressing cells throughout the VNO, we analyzed VNO whole mounts of homozygous V2R-GFP mice by confocal microscopy. The cell bodies of *V2r1b*-expressing neurons are distributed throughout the sensory epithelium of the VNO. There is no obvious preferential distribution of these neurons along the anterior-posterior and dorsal-ventral axes (Figure 1Ca). In coronal sections through the VNO, cell bodies of *V2r1b*-expressing neurons are found in the basal layer of the epithelium, as expected for a member of the V2R family (Figure 1Cb). Labeled neurons are usually found in clusters of two to five cells. No significant difference was found between males and females (data not shown).

Monoallelic expression has been observed both for *OR* genes (Chess et al., 1994; Strotmann et al., 2000; Ishii et al., 2001) and *V1R* genes (Belluscio et al., 1999; Rodriguez et al., 1999). To determine if the *V2R* genes maintain this olfaction-associated trait, we counted the total number of GFP-positive cell bodies in coronal sections through the entire VNO of homozygous and heterozygous V2R-GFP mice. Homozygous mice have approximately twice the number of cells seen in heterozygous mice (237 ± 18 versus 432 ± 49, respectively), suggesting that the *V2r1b* gene is also monoallelicaly expressed. This genetic feature will prove useful for comparison of projection patterns in heterozygous and homozygous mice (see below).

The *V2R2* gene and closely related genes are coexpressed with other *V2R* genes in most VSNs of the basal layer (Martini et al., 2001). In sections of the VNO from V2R-GFP mice, we observe colocalization of the V2R2 antigen with GFP (data not shown). Thus, neurons expressing *V2r1b* also express member(s) of the *V2R2* subfamily, suggesting that *V2r1b* is representative gene of the V2R repertoire.

Pattern of V2r1b-Axonal Projections in the AOB

In the absence of any obvious distribution of *V2r1b*-expressing neurons at the level of the epithelium, we asked if their axons converge to glomeruli in the AOB and whether a spatial distribution of these glomeruli can be discerned.

In whole-mount specimens of V2R-GFP mice analyzed by confocal microscopy ($n = 15$ females and 15 males), V2r1b-axons converge onto six to ten glomeruli per AOB (Figures 2Aa–2Ac), a situation intermediate between that of OSN axons (two to three glomeruli) (Mombaerts, 2001) and that of axons of VSN expressing any of three examined V1R receptors (15–30 glomeruli) (Belluscio et al. 1999; Rodriguez et al., 1999). The V2r1b glomeruli are invariably located in the rostral half of the caudal AOB. Figure 2Ad shows a similar analysis of the AOB of a homozygous mouse of the *VR$_i$2-IRES-tauGFP* strain (Rodriguez et al., 1999), here abbreviated as V1R-GFP. The general glomerular pattern of V2R-GFP mice is established by postnatal day 8 and does not obviously vary with age, gender, or sexual experience. No consistent changes were observed in the number and position of V2r1b glomeruli in sexually naïve versus experienced mice (males and females) (data not shown).

To evaluate better the spatial distribution of the V2r1b glomeruli, we performed three-dimensional reconstructions of sagittal sections through the AOB. This type of analysis (Figures 2Ba–2Bc) revealed common features among the relative depth of the V2r1b glomeruli within the glomerular layer (Figures 2Bd–2Bg) that could not be appreciated in the whole-mount analysis. The one or two most lateral glomeruli are consistently superficial (red) and the remainder are positioned deeper, at the boundaries of the glomerular layer with the external plexiform layer.

Circuit Organization of Glomeruli and Second-Order Neurons

Given that the major output neurons in the AOB, the mitral cells, receive input from multiple glomeruli (Ramon y Cajal, 1911; Takami and Graziadei, 1991) and that VSNs expressing a given VR project to multiple glomeruli, the question is raised as to how the mitral cell connectivity in the AOB relates to glomerular specificity. Three general models can be proposed, each with different functional implications (Figure 3). In the first model, glomeruli are homogeneously innervated by axons of neurons expressing the same receptor, and a given mitral cell connects to those multiple glomeruli that have the same receptor identity (homotypic connectivity). In the second model, glomeruli are also homogeneous at the input level, but a given mitral cell projects its dendrites to glomeruli with different receptor identities (heterotypic connectivity). The third model proposes glomeruli heterogeneously innervated by axons of neurons expressing different receptor types and mitral cells exhibiting a complex pattern of glomerular connectivity (mixed connectivity).

To evaluate these models, we first examined the homogeneity of input to glomeruli in the AOB. It has been shown that V1R glomeruli in the anterior AOB are generally homogeneous at the input level (Belluscio et al., 1999; Rodriguez et al., 1999), with a few exceptions in

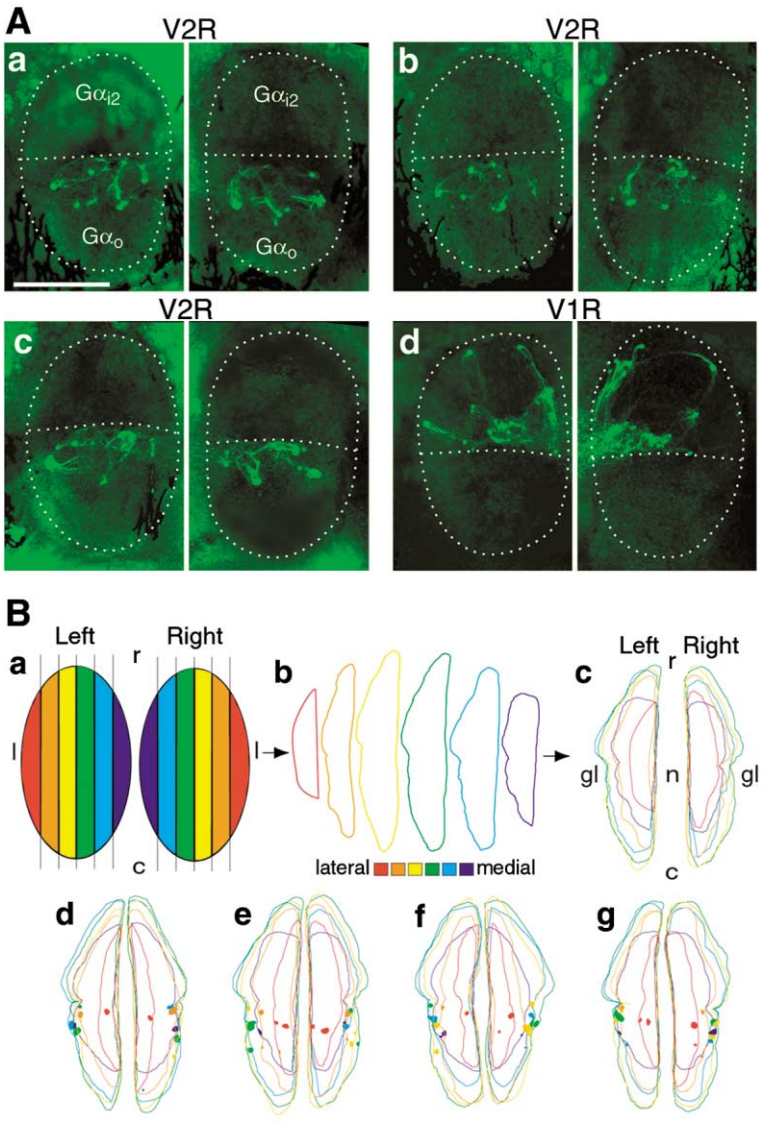

Figure 2. Patterns of Axonal Projections in the Accessory Olfactory Bulb

(A) Whole-mount views of the left and right AOBs.

(Aa–Ac) Five-week-old homozygous V2R-GFP mice. Each AOB has six to ten glomeruli, with a globally conserved spatial distribution (Aa–Ac). (Ad) Five-week-old homozygous V1R-GFP mouse. Each AOB has 15–30 green fluorescent glomeruli in the rostral region. Scale bar, 500 μm.

(Ba–Bg) Three-dimensional reconstruction of sagittal serial sections through the AOB. Cartoon showing the method employed to create three-dimensional reconstructions of serial sections through the AOB (Ba–Bc). (Ba) Dorsal view of the left and right AOBs (same view as in Figure 2A). The six sagittal sections through the AOB are color-coded from lateral to medial: red, orange, yellow, green, blue, purple. The orientation is: r, rostral; c, caudal; l, lateral. (Bb) The six individual serial sagittal sections of the left AOB with the same color coding as in (Ba). Only the nerve and glomerular layers are drawn. Each section is flipped 90° in the horizontal plane such that to the left is the boundary of the glomerular layer and to the right is the boundary of the nerve layer. Top is rostral, and bottom is caudal. (Bc) Illustration of how the sections are reconstructed on top of each other for the left and right AOBs. The orientation of the section is indicated as follows: r, rostral; c, caudal; n, boundary of nerve layer; gl, boundary of glomerular layer. (Bd–Bg) Three-dimensional reconstructions showing the conservation of glomerular distributions in the AOB. Reconstructions of the left and right AOBs of four mice are shown.

which some glomeruli appear to be compartmentalized (Belluscio et al., 1999). With a similar objective, we stained serial sagittal sections of the AOB of homozygous and heterozygous V2R-GFP mice with antibodies against the presynaptic marker synapsin I (Figure 4). We asked whether synaptic markers in each V2r1b glomerulus (red fluorescence) fully correspond with the green fluorescent axons, or whether nongreen fluorescent axons intermingle in the glomerulus. In homozygous V2R-GFP mice, there is a high degree of concordance between synapsin I immunofluorescence and GFP expression, suggesting that only GFP-positive axons in-

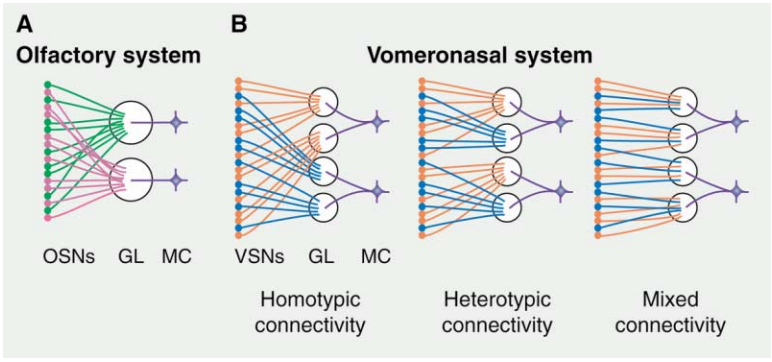

Figure 3. Models of Connectivity in the Main Olfactory and Vomeronasal Systems

(A) In the main olfactory system, axons from OSNs expressing the same OR converge to one (or a few) glomeruli (GL) in the MOB. Mitral cells (MC) send their single apical dendrite to a single glomerulus.

(B) In the vomeronasal system, axons from VSNs expressing the same VR converge to multiple small glomeruli (GL) in the AOB. Mitral cells (MC) have several apical dendrites that innervate multiple glomeruli. Three possible models of connectivity between VSNs and mitral cells are proposed.

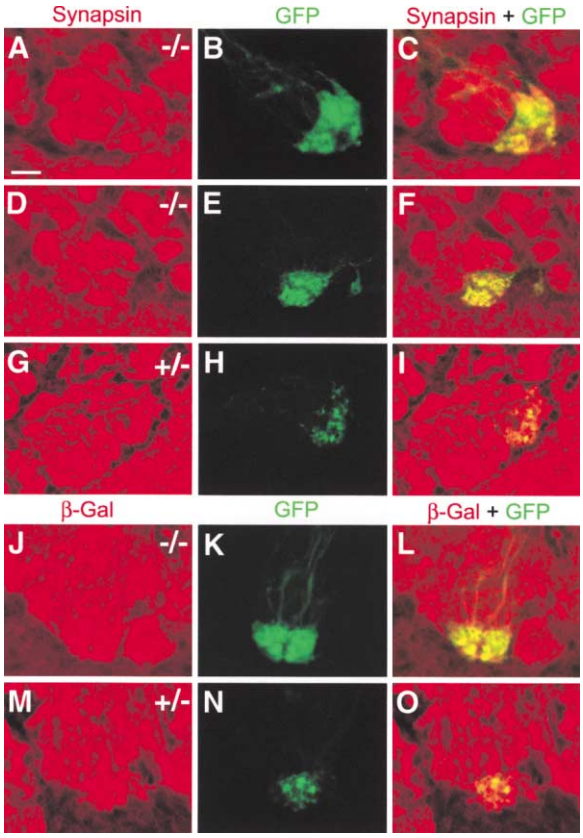

Figure 4. V2r1b-Glomeruli Are Homogeneous at the Input Level

(A–I) Left shows sagittal sections through the AOB of VR2-GFP mice stained with synapsin antiboby (red). Middle contains the same sections and shows the V2r1b green fluorescent glomeruli. Right shows the superimposition of the synapsin antibody staining and the green fluorescence (yellow). (A)–(F), homozygous mouse; (G)–(I), heterozygous mouse. In glomeruli from homozygous mice, the green fluorescence of the V2r1b-axons matches fully with the synapsin antibody staining within the glomerulus. In glomeruli from heterozygous mice, however, the green fluorescence does not fill the glomerular area, as expected if only half of the V2r1b-neurons express GFP from the mutant allele.

(J–O) Left shows sagittal sections through the AOB of V2R-GFP/OMP-taulacZ double mutant mice stained with a β-Gal antiboby (red). Middle contains the same sections and shows V2r1b green fluorescent glomeruli. Right shows the superimposition of the β-Gal antibody staining and the green fluorescence. (J)–(L), homozygous V2R-GFP mouse; (M)–(O), heterozygous mouse. This analysis corroborates that V2r1b-axons fully occupy the glomerular space in the homozygous mice as opposed to heterozygous mice. Scale bar, 10 μm.

nervate these glomeruli (Figures 4A–4F). This was the case for more than 40 analyzed glomeruli of different sizes and shapes. By contrast, nongreen fluorescent patches were observed within the synapsin-I-stained V2r1b glomeruli of heterozygous mice. This is expected because only half of the V2r1b-neurons express GFP due to monoallelic expression of the *V2r1b* gene. Thus, unmarked *V2r1b*-expressing axons could be detected with our method, at least if present in significant numbers. A more definitive analysis of the level of homogeneity of V2r1b glomeruli requires microscopy methods with single axon resolution such as electron microscopy, as we recently applied for glomeruli in the MOB (Treloar et al., 2002).

To extend the finding of the apparently homogeneous innervation of V2r1b glomeruli with a marker specific for VSNs, we crossed V2R-GFP to OMP-taulacZ mice (Mombaerts et al., 1996). The resulting mice express taulacZ in all VSNs and GFP only in V2r1b neurons. Sections through the AOB were stained with antibodies to β-galactosidase. The β-galactosidase-positive axons in V2r1b-glomeruli of homozygous mice were also GFP positive, confirming that these glomeruli are innervated predominantly by V2r1b axons (Figures 4J–4L). In contrast, in heterozygous V2R-GFP mice, a partial overlap was clearly seen (Figures 4M–4O). We repeated this analysis on V1R-GFP mice and confirmed that as we reported before (Rodriguez et al., 1999), VR_i2-glomeruli receive axons of neurons predominantly with that particular receptor identity (data not shown).

These results indicate that glomeruli in both the anterior and posterior AOB are innervated predominantly, if not exclusively, by axons of VSNs expressing the same VR gene, thus excluding the mixed connectivity model (Figure 3B).

Mitral Cells Innervate Glomeruli with the Same VR Specificity

Having shown that V1R and V2R glomeruli receive highly homogeneous inputs, we next asked whether mitral cells connect to glomeruli innervated by axons of VSNs that express the same receptor (homotypic connectivity) or cross-connect glomeruli of different receptor specificities (heterotypic connectivity).

To visualize the mitral cells that connect to glomeruli with a defined receptor identity, we injected GFP-positive glomeruli of either V1R-GFP or V2R-GFP mice with fluorescent lipophilic tracers in AOB slices. The first set of experiments was designed to assess qualitatively whether we could identify mitral cells that connect to several GFP-positive glomeruli. In this experimental design, a single GFP-positive glomerulus was injected with DiI (Figure 5A), and we looked for labeled mitral cell dendrites (that have taken up the dye in the injected GFP-glomerulus) entering other GFP-labeled glomeruli. As illustrated in Figure 5B, DiI-labeled dendrites were observed projecting to other GFP-labeled glomeruli. The figure shows a DiI-labeled dendrite that branches and innervates two GFP-positive glomeruli of a V2R-GFP mouse. In this case, the injection was made into a third glomerulus located about 300 μm laterally to these two (Figure 5A). Figures 5C–5E show high-power views of DiI-labeled dendrites entering the GFP-positive glomerulus. The typical pattern of the dendritic arbor observed within the glomerulus (Takami and Graziadei, 1991) suggests that the labeled dendrites receive synapses from the sensory axons and are not simply passing through the glomerulus. These results show that a given mitral cell can project its dendrites to at least three of the six to ten glomeruli innervated by axons of VSNs that express V2r1b. DiI-labeled dendrites were occasionally observed projecting to non-GFP glomeruli (data not shown). However, labeled dendrites originating from the same mitral cell were never seen innervating both GFP-positive and GFP-negative glomeruli. The labeled den-

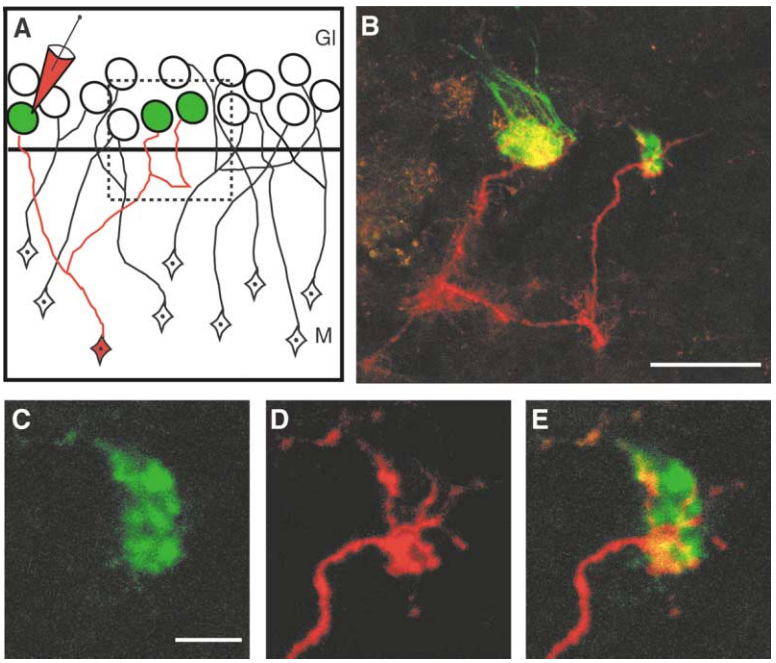

Figure 5. Mitral Cells Can Innervate Multiple Glomeruli with the Same VR Specificity

(A) Diagram illustrating the experimental design and results. A GFP-positive glomerulus at the surface (left) of a thick slice is injected with DiI (red). The dye is taken up by the dendrites of mitral cells innervating that glomerulus and is transported to the dendrites and soma. Labeled dendrites of a mitral cell innervating the injected glomeruli also project to two other GFP-glomeruli that are approximately 300 μm away from the injection site. The thick slice is subsequently cut into thinner sections for confocal analysis.

(B) Dendritic projection from mitral cells labeled with DiI (red) in a GFP-positive glomerulus approximately 300 μm away (and not visible here). The two GFP-positive glomeruli are innervated by labeled dendrites, and thus appear yellow. This means that at least three GFP-positive glomeruli receive dendrites from the same mitral cell. Scale bar, 100 μm.

(C–E) High-power view of the glomerulus in (B), showing a branching labeled apical dendrite penetrating the GFP-positive glomerulus. (C) shows the GFP-glomerulus, (D) shows the labeled apical dendrite, and (E) shows superimposition of both images. Scale bar, 20 μm.

drites entering a GFP-negative glomerulus may result from dye uptake by dendrites that pass through the injected glomerulus without synapsing. Alternatively, they may represent a population of mitral cells with some degree of heterotypic connectivity.

In a second, quantitative set of experiments, pairs of GFP-positive glomeruli from either V1R-GFP or V2R-GFP mice were injected with lipophilic dyes with different wavelength emissions, in tangential slices through the AOB. One slice per AOB was used and each slice contained an average of three to four GFP-positive glomeruli. In slices prepared from both strains of mice, injections were made with DiI into a GFP-positive glomerulus and DiA or DiD into a second GFP-positive glomerulus (Figure 6A). Control experiments were performed in which the second injection was made into a random, GFP-negative glomerulus at a comparable distance. If the same mitral cell innervates both injected glomeruli, its cell body would be labeled with both dyes simultaneously. If mitral cells preferentially project dendrites to multiple glomeruli with the same receptor identity, we would expect to observe double-labeled mitral cells with dendrites projecting simultaneously to both GFP-positive injected glomeruli at a frequency higher than when a GFP-positive and a random GFP-negative glomerulus are injected. Indeed, the percentage of double-labeled mitral cells observed when two GFP-labeled glomeruli were injected was significantly higher than when a GFP and a non-GFP glomerulus were injected (Figure 6B). The absolute percentage of double- versus single-labeled mitral cells within each double-injection experiment is not informative in this experimental design because a high number of single-labeled mitral cells is expected for at least two reasons. First, some mitral cells will innervate some of the other GFP-positive glomeruli that reside in the slice but were not injected or that reside outside the slice. Second, some mitral cells may project their dendrite(s) to only a single glomerulus.

Figures 6C and 6E show V2R-GFP and V1R-GFP glomeruli that were injected with DiI and DiD, respectively: injections were controlled such that each was strictly confined to the GFP-positive glomeruli. Figures 6D and 6F depict resulting double- and single-labeled mitral cells from an injection in an AOB slice of V2R-GFP and V1R-GFP mice, respectively.

Taken together, these findings suggest that mitral cells in both rostral and caudal AOB tend to project their dendrites to glomeruli that receive input from VSNs expressing the same receptor, thereby reorganizing the dispersed glomerular inputs into a more convergent pattern.

Discussion

The Functional Anatomy of the Olfactory System

In most mammals, two sensory systems have evolved to mediate distinct biological responses to chemical compounds: the main olfactory and vomeronasal systems. While significant progress has been made in our knowledge of the main olfactory system, progress in our understanding of the vomeronasal system has been slow. The functional organization of the sensory neurons and their first synaptic relay station in the vomeronasal pathway differ from the main olfactory system in two aspects: first, axons of VSNs expressing the same V1R project to multiple glomeruli (Belluscio et al., 1999; Rodriguez et al., 1999), and second, dendrites of second-order neurons innervate multiple glomeruli (Ramon y Cajal, 1911; Takami and Graziadei, 1991).

To reveal the wiring logic of the vomeronasal system, we have described the pattern of axonal projections of VSNs expressing a given *V2R* gene to glomeruli and

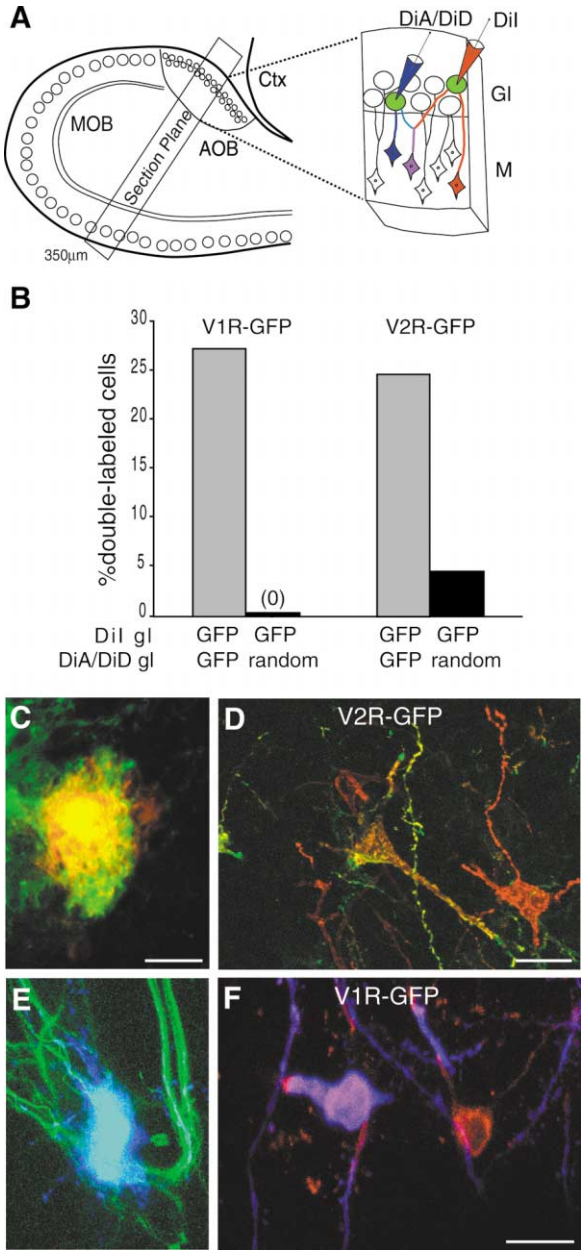

Figure 6. Mitral Cell Dendrites Tend to Project to Glomeruli With the Same VR Identity

(A) Diagram showing slice section plane through the AOB and the resulting slice, with (GI) and mitral cell (M) layers. The experimental design is illustrated for an injection with DiD (blue) and DiI (red). Each dye is injected into one of two GFP-positive glomeruli in the slice. Dendrites of mitral cells innervating this glomerulus take up the dye, which is transported to the soma. Mitral cells that send dendrites to both glomeruli show colocalization of both dyes in their cell bodies (pink); mitral cells that send dendrites to only one of two GFP-positive glomeruli have a single dye in their soma (either blue or red).

(B) Double-injection experiments. The vertical axis depicts the percentage of the total number of double-labeled mitral cells over the total number of labeled mitral cells for all the experiments performed in each group. The total number of labeled mitral cells per experiment was taken as the average number of cells labeled with DiI and DiA/DiD. Gray bars represent experiments in which each dye (DiI and DIA or DiD) is injected into one of two GFP-labeled glomeruli (n = 6 slices for V1R-GFP and n = 7 slices for V2R-GFP). Black bars represents experiments in which a first dye is injected into a GFP-labeled glomerulus and the second dye in a randomly chosen glomerulus, at distances to the first injected glomeruli comparable to the distances of other GFP-labeled glomeruli in the slice (n = 3 slices for V1R-GFP and n = 4 slices for V2R-GFP). The total number of labeled cells for the GFP-GFP glomerular injections was 73 for V1R-GFP and 65 for V2R-GFP; of these, 20 cells were double labeled in V2R-GFP mice (27.4%) and 16 cells in V2R-GFP mice (24.6%). For the GFP-random glomerular injections, the total number of labeled cells was 11 for V1R-GFP and 44 for V2R-GFP; 0 cells were double labeled in V2R-GFP (0%) and 2 cells in V2R-GFP (4.5%). For both V1R-GFP and V2R-GFP, the percentage of double-labeled mitral cells in the GFP-GFP injections is significantly higher than that in the GFP-random injections, with $p = 0.044$ and $p = 0.004$, respectively, as evidenced with the Fisher's Exact test.

(C) DiI (red) injection site in a slice of the AOB of a V2R-GFP mouse. The core of the injection site is situated in the center of the GFP-positive glomerulus (green). The overlay results in a yellow color. Scale bar, 20 μm for (C) and (D).

(D) Mitral cell labeled by both DiA (green) and DiI (red) (left cell) and a mitral cell labeled by DiI alone (right cell) in V2R-GFP AOB. Scale bar, 20 μm.

(E) DiD (blue) injection site in a V1R-GFP AOB. The core of the injection is restricted to the GFP-positive glomerulus. The overlay results in a light-blue color.

(F) A DiD/DiI double-labeled mitral cell (left, pink) and a DiI-only labeled mitral cell (right cell, red) in the AOB of a V1R-GFP mouse. Scale bar, 20 μm.

analyzed the pattern of connectivity between defined sets of glomeruli and second-order output neurons in the AOB. We show that the organization of the two pathways in the vomeronasal system follows similar principles, although the repertoires of putative chemosensory receptors employed by these pathways share no sequence similarity. Axons of neurons expressing a given V1R or V2R converge onto multiple glomeruli in the AOB that receive homogeneous input from neurons expressing the same receptor, with some exceptions of apparently compartmentalized glomeruli (Belluscio et al., 1999). Within each subdivision of the AOB, a given mitral cell sends dendrites that terminate in multiple glomeruli innervated by neurons expressing the same receptor. Thus, the functional organization of the vomeronasal system is more convergent than originally thought. The apparent divergent axonal connectivity of VSNs to the AOB is reorganized by the dendrites of the second-order neurons into a more convergent output pattern, similar to that observed in the MOB.

Glomerular Patterns in the AOB

The patterns of glomeruli innervated by neurons expressing a given V1R or V2R have both conserved and variable features. While V1R or V2R glomeruli are distributed in broadly conserved areas of the AOB, their precise locations vary across individuals and between both bulbs of the same individual.

Although we have described the expression and projection patterns for only one gene of a repertoire of ~140 *V2R* genes (Matsunami and Buck, 1997), experience with both OR genes and *V1R* genes has shown that the basic theme of these patterns appears to be generalizable based on one or a few randomly chosen gene members. Nonetheless, certain characteristics vary across the neuronal populations studied, such as the dependency

of the glomerular MOB pattern on an active cyclic nucleotide-gated channel (Zheng et al., 2000) and the heterogeneity of V1R-axonal projections in a subset of larger AOB glomeruli (Belluscio et al., 1999). Genetic tagging of additional *V2R* genes will be required to test the generality of our findings.

The evidence for rigid locations of glomeruli in the MOB is biased by the small number of glomeruli that are associated with a given OR. Recently, it has become clear that the position of glomeruli for a given OR is not as fixed and invariable as originally thought. Instead local permutations can be discerned within an area of ~30 glomeruli (Strotmann et al., 2000; Schaefer et al., 2001). If the same extent of variability for individual glomeruli is extended to 6–30 glomeruli instead of a few, the variability of the glomerular patterns would become more pronounced. Thus, it remains to be determined to what extent spatial uncertainty differs between the MOB and AOB at the level of the individual glomerulus.

Homotypic Connectivity

It has been known for nearly a century (Ramon y Cajal, 1911) and was shown later in greater detail (Takami and Graziadei, 1990, 1991) that AOB mitral cells project their apical dendrites to multiple glomeruli. The number of apical dendrites per mitral cell is variable, with some cells having only one apical dendrite while others up to six (Takami and Graziadei, 1990, 1991). This particular dendritic projection pattern of mitral cells, combined with the multiple projections sites of neurons with the same V1R specificity, has led to the proposal of different models for the connectivity of these two neuronal populations in the AOB (Keverne, 1999) (Figure 5).

The first model (homotypic connectivity) proposes that each glomerulus receives input only from neurons expressing the same VR and that a given mitral cell projects its dendrites to glomeruli with the same receptor identity. In this model, a convergence of receptor information is achieved by the second-order neurons, the mitral cells. The second model (heterotypic connectivity) also considers that glomeruli are innervated homogeneously by neurons with the same VR specificity, but a given mitral cell projects its dendrites to glomeruli with different receptor identities. This model assigns a key role to mitral cells in integrating information from different receptor types. In the third model (mixed connectivity), the glomeruli are innervated by intermingling axons of neurons expressing different receptor types and mitral cells receive inputs from multiple mixed glomeruli.

We observe that V1R- or V2R-specific glomeruli are innervated predominantly, if not exclusively, by axons of sensory neurons expressing the same receptor type and that mitral cells tend to project their dendrites to glomeruli with the same VR specificity. These results support the first model, that of homotypic connectivity. The observation that some V1R glomeruli may exhibit compartmentalization (Belluscio et al., 1999) does not preclude such organization: the spatial segregation of axons from neurons expressing the same V1R within a compartmentalized glomerulus could match the apical dendrites of a specific mitral cell.

Our results suggest an organization of sensory axons and mitral cell dendrites based on receptor specificity. We cannot exclude the possibility that some degree of cross-connection to glomeruli with different VR specificities occur. However, it must be a rare event, as evidenced by the low percentage of mitral cells that project to both GFP-positive and GFP-negative glomeruli. We cannot exclude either a highly organized pattern of connectivity in which mitral cells preferentially connect glomeruli with the same VR specificity but also project to other glomeruli with a different but particular VR specificity. Because random glomeruli were injected in the control experiments, this possibility could not be evaluated. Injection of fluorescent tracers into individual mitral cells would be required to evaluate these possibilitites. However, this faces the technical difficulty of identifying a population of mitral cells projecting to GFP-labeled glomeruli.

Axonal Divergence and Dendritic Convergence

A circuit organization in which mitral cells receive inputs from the same type of VSNs resembles that of the main olfactory system in which mitral cells receive inputs from a single glomerulus. The two systems thus may use a similar general computational scheme, with a convergence of receptor-specific sensory inputs onto a small population of output neurons. This convergence is achieved at the level of glomeruli in the MOB and at the level of the mitral cells in the AOB.

Why would the vomeronasal system be structured in such a way that there is first divergence of information into multiple glomeruli followed by convergence at the level of the mitral cells? One possibility is that there are no significant functional advantages to the distributed arrangement of glomeruli but that this arrangement results as a consequence of a set of developmental restrictions different from those operating on the MOB. If the high convergence of axons from neurons expressing the same receptor in the MOB is mainly a consequence of developmental wiring efficiency and if this constraint is less stringent in the AOB, then a more divergent pattern of sensory axonal projections could be expected. If the convergence of receptor type information is critical for the coding of olfactory information, it can as well be achieved at the level of the output neurons instead of at the level of the glomeruli. Alternatively, the distributed arrangement of glomeruli may reflect a unique function of the vomeronasal system, such as extracting information about concentration features of the different compounds in a pheromone blend. Another possibility is that the formation of multiple glomeruli of the same receptor type may be important for enhancing signal to noise via glomerular level lateral inhibition. Multiple small glomeruli of the same type are adjacent to a greater number of other receptor type glomeruli than a single large glomerulus, as the surface area is greatly increased. Thus, the ensemble of the multiple glomeruli of the same receptor type has the potential for more extensive and more diverse lateral inhibition compared to a single glomerulus of larger size.

Distinct functional implications result from a scenario in which mitral cells preferentially connect to glomeruli innervated by neurons expressing the same receptor but also connect to some other glomeruli with different

but, perhaps, particular receptor specificities. In this case, each mitral cell collects information resulting from the activation of the same receptor type, but this would be read in the context of the concurrent activation of the glomerulus (or glomeruli) with a different receptor identity. This arrangement could be advantageous for decoding pheromonal information in an odor mixture of components that need to be present in a critical ratio of concentrations (Hildebrand, 1995). Mitral cells may sense the relative concentration of two compounds in a blend by computing the relative activation of the glomeruli of the same receptor identity vis-à-vis those with other receptor identities. However, such a model would require mitral cell dendrite connectivity between different glomeruli to precisely match biologically relevant pheromone blends, an enormous problem of specificity.

How do dendrites of the same mitral cell specifically innervate glomeruli with the same VR identity? This is another formidable wiring problem. It is possible that dendritic connections may be first widespread over many glomeruli with different receptor specificities and be later refined by activity-dependent pruning of inappropriate connections. Only those dendrites that are activated concurrently could survive. Conversely, a matching set of guidance molecules expressed by mitral cells could specifically recognize each population of axons carrying a different vomeronasal receptor.

Experimental Procedures

Targeted Mutagenesis of the *V2r1b* Gene

A 9 kb EcoRI fragment containing the transmembrane domain exon and 3′ nontranslated region of the *V2r1b* gene was subcloned in pBluescript from a Stratagene 129/Sv genomic library in λFIX by Nicholas Ryba (NIH) and kindly provided to us. A portion of the intron region 5′ to the transmembrane domain exon was isolated by PCR from the 9 kb fragment subclone and used as a probe to screen a 129/Sv genomic BAC library (Genome Systems). Determining the sequence of the six exons spanning the *V2r1b* coding region and of the intron-exon boundaries revealed a complete open reading frame and conserved splice sites. The sequence corresponded to that of the *V2r1b* cDNA cloned by Ryba, excluding that it is a pseudogene. This analysis was of particular importance because of the high proportion of pseudogenes reported for the *V2R* family (Herrada and Dulac, 1997; Matsunami and Buck, 1997).

A 7.5 kb Kpn-EcoR1 fragment containing exon 6 of the *V2r1b* gene was used to engineer the targeting vector. A PacI site was generated by recombinant PCR immediately after the stop codon of *V2r1b*. The *IRES-tauGFP-LNL* cassette (Rodriguez et al., 1999) was inserted in this PacI site to assemble the *V2r1b-IRES-tauGFP* targeting vector.

Targeting vectors were linearized with AscI. Electroporation and cell culture of embryonic day (E)14 cells were carried out as described before (Mombaerts et al., 1996). Genomic DNA from G418-resistant ES clones was digested with EcoR1 and homologous recombinant clones were identified by Southern blot hybridization with a 5′ probe external to the targeting vector. One of these clones was introduced into blastocysts to generate chimeric mice from which germline transmission was obtained.

The *neo*-selectable marker was removed from the targeted mutation by crossing mice heterozygous for the *LNL* allele to *Ella-Cre* transgenic mice (Lakso et al., 1996). Transgenic mice used were backcrossed by us at least four times to the C57BL/6 background. Intercrossing of the *loxP*-positive mice resulted in *loxP* heterozygous and *loxP* homozygous mice that were devoid of the *Cre* transgene. All analyses were performed with mice that did not carry the *Cre* transgene. Mice are in a mixed (129 × C57BL/6) background. Mice carrying the *V2r1b-IRES-tauGFP* targeted mutation (strain V1G180) are termed V2R-GFP.

Tissue Preparation and Whole-Mount Analysis

Deeply anesthetized V2R-GFP mice were transcardially perfused with 4% paraformaldehyde in PBS (pH 7.4). The VNOs and brains were postfixed in the same fixative for 1 hr and then transferred to 30% sucrose in PBS for 48 hr at 4°C. Whole mounts were imaged using a Zeiss confocal microscope and 8–15 Z stacks were acquired every 8–9 μm. The resulting stacks were reconstructed manually in Adobe Photoshop.

Three-Dimensional Reconstructions

AOBs from more than 20 mice were serially sectioned in a sagittal plane at 50 μm using a freezing sliding microtome (Leica). Sections were stained with DAPI to allow identification of the glomerular layer. Images were taken for each section with a Digital camera (SPOT-RT, Diagnostic Instruments) attached to a fluorescence microscope (Zeiss Axioskop II). Boundaries of the AOB and glomerular layer and glomeruli in each section were drawn with CorelDraw. Each serial section was given a different color, from lateral to medial, and the sections were reconstructed on top of each other, aligning them with the outer border of the nerve layer.

Immunohistochemistry

VNOs were sectioned coronally, using a freezing sliding microtome (Leica) and AOBs sagittally at 20–40 μm thickness. VNO sections were mounted onto slides for immunostaining while AOBs were stained as free-floating sections. Sections were treated according to standard free-floating immunohistochemistry protocols. For synapsin I staining, an antibody generated against the C terminus of synapsin 1a (G304) was provided by Paul Greengard (The Rockefeller University) and used at 1:1000. This antibody recognizes mouse synapsin 1a, 2a, and 3a. A rabbit anti-V2R2 antibody (Martini et al., 2001) was provided by Roberto Tirindelli (University of Parma, Italy) and used at 1:500. For β-galactosidase immunohistochemistry, a rabbit IgG fraction (Cappel) was used in a 1:100 dilution. An anti-rabbit secondary antibody conjugated to Cy3 was used to visualize where the primary antibodies bound (Jackson ImmunoResearch). Immunostained sections were imaged using a Zeiss confocal microscope and Z stacks were acquired every 1–2 μm.

Glomerular Injections with Fluorescent Dyes

Vibratome sections (350 μm) were cut in a horizontal plane through the AOB (approximately 35° from coronal plane). These slices pass through the center of the AOB perpendicular to the glomerular layer and contain all layers of the AOB in cross-section. Each slice comprises approximately 25%–35% of the AOB and contains three to four GFP-positive glomeruli per AOB. A single slice per AOB was used. Each slice was maintained in constant flow oxygenated artificial cerebrospinal fluid (120 mM NaCl, 3 mM KCl, 1.3 mM $CaCl_2$, 1.3 mM $MgSO_4$, 25 mM NaH_2CO_3, 10 mM glucose, and 5 mM BES) at 30°C–32°C on an upright microscope fitted with a long working distance 40× water immersion objective and fluorescence. Micropipettes (1.5 μm tip) containing either DiI, DiA, or DiD were guided visually into GFP glomeruli using an hydraulic micromanipulator and a small (5–10 μm) iontophoretic injection made. For control experiments, the double injections were made at similar distances as for the two GFP-positive glomeruli. In general, injected glomeruli were 100–150 μm apart. Slices were fixed with 4% paraformaldehyde in 0.1 M phosphate-buffered saline (pH 7.4) for 1 hr and then transferred to 1% paraformaldehyde in 0.1 M phosphate-buffered saline (pH 7.4) for 24–48 hr. These 350 μm sections were resectioned at 50 μm on a vibratome, mounted in a DABCO (Sigma) based anti-fade mounting media, and optically sectioned on a FluoView confocal microscope (Olympus Instruments). The proportions of mitral cells were counted in slices that contained at least two labeled mitral cells in both injections.

Acknowledgments

We are grateful to Ruben Peraza and Annemarie Walsh from the Transgenic Service at The Rockefeller University for generating chimeric mice. We thank Tom Bozza, Stuart Firestein, Charlie Greer, and Leslie Vosshall for useful comments on the manuscript. A.C.P. was supported by National Institutes of Health grant DC000347. I.R.

was supported by the Swiss National Foundation for Research. P.M. received grant support from the March of Dimes Birth Defects Organization and the National Institutes of Health.

Received: April 23, 2002
Revised: August 14, 2002

References

Belluscio, L., Koentges, G., Axel, R., and Dulac, C. (1999). A map of pheromone receptor activation in the mammalian brain. Cell *97*, 209–220.

Berghard, A., and Buck, L.B. (1996). Sensory transduction in vomeronasal neurons: evidence for Gαo, Gαi2, G, and adenlylyl cylcase II as major components of a pheromone signaling cascade. J. Neurosci. *16*, 909–918.

Brennan, P.A., Schellinck, H.M., and Keverne, E.B. (1999). Patterns of expression of the immediate-early gene egr-1 in the accessory olfactory bulb of female mice exposed to pheromonal constituents of male urine. Neuroscience *90*, 1463–1470.

Bozza, T., Feinstein, P., Zheng, C., and Mombaerts, P. (2002). Odorant receptor expression defines functional units in the mouse olfactory system. J. Neurosci. *22*, 3033–3043.

Buck, L., and Axel, R. (1991). A novel multigene family may encode odorant receptors: a molecular basis for odor recognition. Cell *65*, 175–187.

Chess, A., Simon, I., Cedar, H., and Axel, R. (1994). Allelic inactivation regulates olfactory receptor gene expression. Cell *78*, 823–834.

Del Punta, K., Rothman, A., Rodriguez, I., and Mombaerts, P. (2000). Sequence diversity and genomic organization of vomeronasal receptor genes in the mouse. Genome Res. *10*, 1958–1967.

Dudley, C.A., and Moss, R.L. (1999). Activation of an anatomically distinct subpopulation of accessory olfactory bulb neurons by chemosensory stimulation. Neuroscience *91*, 1549–1556.

Dulac, C., and Axel, R. (1995). A novel family of genes encoding putative pheromone receptors in mammals. Cell *83*, 195–206.

Firestein, S. (2001). How the olfactory system makes sense of scents. Nature *413*, 211–218.

Halem, H.A., Baum, M.J., and Cherry, J.A. (2001). Sex difference and steroid modulation of pheromone-induced immediate early genes in the two zones of the mouse accessory olfactory system. J. Neurosci. *21*, 2474–2480.

Halpern, M. (1987). The organization and function of the vomeronasal system. Annu. Rev. Neurosci. *10*, 325–362.

Halpern, M., Shapiro, R.S., and Jia, C. (1995). Differential localization of G proteins in the opossum vomeronasal system. Brain Res. *677*, 157–161.

Herrada, G., and Dulac, C. (1997). A novel family of putative pheromone receptors in mammals with a topographically organized and sexually dimorphic distribution. Cell *90*, 763–773.

Hildebrand, J.G. (1995). Analysis of chemical signals by nervous systems. Proc. Natl. Acad. Sci. USA *92*, 67–74.

Holy, T.E., Dulac, C., and Meister, M. (2000). Responses of vomeronasal neurons to natural stimuli. Science *28*, 1569–1572.

Ishii, T., Serizawa, S., Kohda, A., Nakatani, H., Shiroishi, T., Okumura, K., Iwakura, Y., Nagawa, F., Tsuboi, A., and Sakano, H. (2001). Monoallelic expression of the odourant receptor gene and axonal projection of olfactory sensory neurones. Genes Cells *6*, 71–78.

Jia, C., and Halpern, M. (1996). Subclasses of vomeronasal receptor neurons: differential expression of G proteins ($G_{i\alpha 2}$ and $G_{o\alpha}$) and segregated projections to the accessory olfactory bulb. Brain Res. *719*, 117–128.

Jia, C., and Halpern, M. (1997). Segregated populations of mitral/tufted cells in the accessory olfactory bulb. Neuroreport *8*, 1887–1890.

Keverne, E.B. (1999). The vomeronasal organ. Science *286*, 716–720.

Kumar, A., Dudley, C.A., and Moss, R.L. (1999). Functional dichotomy within the vomeronasal system: distinct zones of neuronal activity in the accessory olfactory bulb correlate with sex-specific behaviors. J. Neurosci. *19*, RC32.

Lakso, M., Pichel, J.G., Gorman, J.R., Sauer, B., Okamoto, Y., Lee, E., Alt, F.W., and Westphal, H. (1996). Efficient in vivo manipulation of mouse genomic sequences at the zygote stage. Proc. Natl. Acad. Sci. USA *93*, 5860–5865.

Leinders-Zufall, T., Lane, A.P., Puche, A.C., Ma, W., Novotny, M.V., Shipley, M.T., and Zufall, F. (2000). Ultrasensitive pheromone detection by mammalian vomeronasal neurons. Nature *405*, 792–796.

Malnic, B., Hirono, J., Sato, T., and Buck, L.B. (1999). Combinatorial receptor codes for odors. Cell *96*, 713–723.

Martini, S., Silvotti, L., Shirazi, A., Ryba, N.J.P., and Tirindelli, R. (2001). Coexpression of putative pheromone receptors in the sensory neurons of the vomeronasal organ. J. Neurosci. *17*, 843–848.

Matsunami, H., and Buck, L.B. (1997). A multigene family encoding a diverse array of putative pheromone receptors in mammals. Cell *90*, 775–784.

Mombaerts, P. (2001). How smell develops. Nat. Neurosci. *4*, 1192–1998.

Mombaerts, P., Wang, F., Dulac, C., Chao, S.K., Nemes, A., Mendelsohn, M., Edmondson, J., and Axel, R. (1996). Visualizing an olfactory sensory map. Cell *87*, 675–686.

Potter, S.M., Zheng, C., Koos, D.S., Feinstein, P., Fraser, S.E., and Mombaerts, P. (2001). Structure and emergence of specific olfactory glomeruli in the mouse. J. Neurosci. *21*, 9713–9723.

Ramon y Cajal, S. (1911). Histologie du systeme nerveux de l'homme et des vertébrés. Reprinted by Consejo Superior de Investigaciones Cientificas, Madrid, 1955 edition (Paris: Maloine).

Ressler, K.J., Sullivan, S.L., and Buck, L.B. (1994). Information coding in the olfactory system: evidence for a stereotyped and highly organized epitope map in the olfactory bulb. Cell *79*, 1245–1255.

Rodriguez, I., Feinstein, P., and Mombaerts, P. (1999). Variable patterns of axonal projections of sensory neurons in the mouse vomeronasal system. Cell *97*, 199–208.

Rodriguez, I., Del Punta, K., Rothman, A., Ishii, T., and Mombaerts, P. (2002). Multiple new and isolated families within the mouse superfamily of V1R vomeronasal receptors. Nat. Neurosci. *5*, 134–140.

Ryba, N.J.P., and Tirindelli, R. (1997). A new multigene family of putative pheromone receptors. Neuron *19*, 371–379.

Sam, M., Vora, S., Malnic, B., Ma, W., Novotny, M.V., and Buck, L.B. (2001). Odorants may arouse instinctive behaviours. Nature *412*, 142.

Schaefer, M.L., Finger, T.E., and Restrepo, D. (2001). Variability of position of the P2 glomerulus within a map of the mouse olfactory bulb. J. Comp. Neurol. *30*, 351–362.

Strotmann, J., Conzelmann, S., Beck, A., Feinstein, P., Breer, H., and Mombaerts, P. (2000). Local permutations in the glomerular array of the mouse olfactory bulb. J. Neurosci. *20*, 6927–6938.

Takami, S., and Graziadei, P.P. (1990). Morphological complexity of the glomerulus in the rat accessory olfactory bulb–a Golgi study. Brain Res. *510*, 339–342.

Takami, S., and Graziadei, P.P. (1991). Light microscopic Golgi study of mitral/tufted cells in the accessory olfactory bulb of the adult rat. J. Comp. Neurol. *311*, 65–83.

Treloar, H.B., Feinstein, P., Mombaerts, P., and Greer, C.A. (2002). Specificity of glomerular targeting by olfactory sensory axons. J. Neurosci. *22*, 2469–2477.

Vassar, R., Chao, S.K., Sitcheran, R., Nuñez, J.M., Vosshall, L.B., and Axel, R. (1994). Topographic organization of sensory projections to the olfactory bulb. Cell *79*, 981–991.

von Campenhausen, H., Yoshihara, Y., and Mori, K. (1997). OCAM reveals segregated mitral/tufted cell pathways in developing accessory olfactory bulb. Neuroreport *8*, 2607–2612.

Yoshihara, Y., Kawasaki, M., Tamada, A., Fujita, H., Hayashi, H., Kagamiyama, H., and Mori, K. (1997). OCAM: A new member of the neural cell adhesion molecule family related to zone-to-zone projection of olfactory and vomeronasal axons. J. Neurosci. *17*, 5830–5842.

Zheng, C., Feinstein, P., Bozza, T., Rodriguez, I., and Mombaerts, P. (2000). Peripheral olfactory projections are differentially affected in mice deficient in a cyclic nucleotide-gated channel subunit. Neuron *26*, 81–91.